

PoisHygiene: Detecting and Mitigating Poisoning Attacks in Neural Networks

Junfeng Guo[†], Zelun Kong[†] and Cong Liu[†]

[†]The University of Texas at Dallas

ABSTRACT

The black-box nature of deep neural networks (DNNs) facilitates attackers to manipulate the behavior of DNN through data poisoning. Being able to detect and mitigate poisoning attacks, typically categorized into backdoor and adversarial poisoning (AP), is critical in enabling safe adoption of DNNs in many application domains. Although recent works demonstrate encouraging results on detection of certain backdoor attacks, they exhibit inherent limitations which may significantly constrain the applicability. Indeed, no technique exists for detecting AP attacks, which represents a harder challenge given that such attacks exhibit no common and explicit rules while backdoor attacks do (i.e., embedding backdoor triggers into poisoned data).

We believe the key to detect and mitigate AP attacks is the capability of observing and leveraging essential poisoning-induced properties within an infected DNN model. In this paper, we present **PoisHygiene**, the first effective and robust detection and mitigation framework against AP attacks. **PoisHygiene** is fundamentally motivated by Dr. Ernest Rutherford’s story (i.e., the 1908 Nobel Prize winner), on observing the structure of atom through random electron sampling. Specifically, **PoisHygiene** crafts multiple random samples as inputs to a given DNN, seeking to reveal necessary internal properties of the decision region space belonging to each label, and then leverage observed properties to detect whether a label is infected. Through extensive implementation and evaluation of **PoisHygiene** against a set of state-of-the-art AP attacks on five widely studied datasets, **PoisHygiene** proves to be effective and robust under various settings considering complex attack variants. Interestingly, **PoisHygiene** is also shown to be effective and robust on detecting backdoor attacks, particularly comparing to the state-of-the-art backdoor detection methods Neural Cleanse and ABS.

1 INTRODUCTION

Deep Neural Networks (DNNs) are being deployed in a myriad of application domains, such as image classification [30], object recognition [39], and security-critical ones including binary reverse engineering [18], malware detection [12, 50], and autonomous driving [15]. DNNs can even exceed human accuracy in many such applications, at the cost of high computational complexity due to training through a large amount of data for obtaining an effective input space representation. Thus, instead of training a DNN model from scratch, users often download trained state-of-the-art DNNs from third-party supply chain such as Model Zoo [8], Gradient Zoo [7], Pytorch Hub [10], which provide well-trained models uploaded by developers.

Unfortunately, the black-box nature of such shared DNN models may enable attackers to manipulate the model through data poisoning, which seeks to manipulate the behavior of DNN via inserting poisoned samples during training [17, 24, 28, 33, 42]. Poisoning attacks have received a good amount of recent attention from both academia and industry, which can be generally categorized into backdoor attacks [17, 19, 24, 33, 52] and adversarial poisoning (AP) attacks [28, 41, 42, 44] (also discussed in [49]). A key difference is that backdoor attacks seek to attach specific triggers to training instances, which override normal classification to produce incorrect prediction results; while AP attacks aim at either simply mis-labeling training data or inserting poisoned instances containing manipulated features that belong to a class different from the original one (note that such features do not need to form a unified pattern as required by the trigger implementation under backdoor attacks).

Compared to designing poisoning attack techniques, detection on such attacks is known to be a much harder problem [17, 49]. A recent set of works focus on detecting backdoor attacks [14, 34, 36, 41]), yet assuming the defender can access the original poisoned instances used during training, which is unfortunately impractical [17, 24, 33]. Recent works, i.e., Neural Cleanse [49] and ABS [32], take significant steps in the direction of detection on backdoor attacks in the image classification domain, which doesn’t require such strong defender capability. The intuitive ideas behind Neural Cleanse [49] and ABS [32] are through observing and exploiting properties unique to certain backdoor attacks (backdoor trigger size for Neural Cleanse and compromised neurons representing the features of backdoor triggers for ABS), thus constraining the applicability to AP attacks.

We believe for any detection method on AP attacks to be effective and robust, it has to be capable of observing and leveraging unique poisoning-induced properties within an infected DNN model (instead of properties specific to certain attack techniques), which is clearly challenging. The challenges are due to the fact that it is rather difficult to observe internal properties of DNN (infected or not) due to its black-box nature, and to leverage such properties in developing effective detection methods against AP attacks which do not exhibit any common and explicit rules in the crafted poisoned data (unlike backdoor triggers).

In this paper, we present **PoisHygiene**, the first detection and mitigation framework against AP attacks. **PoisHygiene** detects infected DNNs via observing and exploring an essential property of any infected DNN model due to poisoning, i.e., the existence of a poisoned decision region w.r.t. each infected label. **PoisHygiene** is fundamentally motivated by Dr. Ernest Rutherford’s story (i.e., the 1908 Nobel Prize winner) [1], on seeking the structure and content of atom through random electron sampling. Similarly, **PoisHygiene** crafts multiple random samples (sampled from Gaussian distribution) as inputs to a given DNN, seeking to reveal essential internal

Conference'17, July 2017, Washington, DC, USA properties of the decision region space belonging to each label. A set of interesting empirically-proved observations on properties of decision regions belonging to a label under two settings where the label is infected or clean (see Sec. 4.1) motivate our key detection criteria.

Through extensive implementation and evaluation of Poishygiene against three state-of-the-art AP attacks [42, 44] on five widely studied datasets, Poishygiene proves to be effective and robust under various settings. Rather interestingly, Poishygiene is also shown to be effective against state-of-the-art backdoor attacks [17, 24, 33]. Such efficacy is particularly demonstrated via direct comparison against Neural Cleanse and ABS on detection against backdoor attacks for several complex attack variants. Such generality is intuitive as Poishygiene's detection criteria is developed through exploring essential properties of any poisoned decision region space, which may hold for both AP and backdoor infected labels.

In summary, this paper makes the following contributions.

- We present effective detection and mitigation techniques against state-of-the-art AP attacks, which are proved to be effective by extensive experiments.
- Evaluation also demonstrates the efficacy of Poishygiene against existing backdoor attacks, particularly comparing to the state-of-the-art backdoor detection methods Neural Cleanse [49] and ABS [32] (e.g., under the multi-infected-label setting).
- Poishygiene is shown to be robust when considering a set of complex attack variants under both AP and backdoor attacks.

To the best of our knowledge, this work is the first to develop robust detection and mitigation techniques against AP attacks (e.g., Sting Ray [44] and Poison Frog [42]), which could not be resolved using any existing defense techniques.

2 BACKGROUND AND RELATED WORK

Due to lack of transparency, DNNs are often treated as black-box systems. A DNN model takes an input (e.g. an image) and then gives a prediction label after performing a series of internal computations. **Poisoning attacks.** Poisoning attacks on DNNs are typically categorized into backdoor attacks and AP attacks [49], both of which have received a significant amount of recent attention [16, 31, 33, 42, 43, 49, 51]. Backdoor attack on DNNs is defined to be training a backdoor trigger (e.g., a small white square) into a DNN, causing anomalous behaviors when the specific trigger is attached into a test-time input. [17, 24, 33]. An advantage of backdoor attacks is that they do not affect overall classification accuracy on clean input data. On the other hand, AP attack techniques seek to maliciously train a DNN using data of certain classes whose features are inconsistent with their assigned labels. Thus, at test time, the classification result on unmodified test data of those specific classes would be incorrect (e.g., a stop sign would be mis-classified as a speed limit sign) [42, 44]. AP attacks can be further categorized into integrity attack [42, 44] and availability attack [13, 28, 41]. Integrity attack aims at causing specific mis-predictions at test time while preserving overall accuracy performance. Availability attack seeks to lower the overall accuracy performance.

Regarding AP attacks, this paper focuses on integrity attacks since availability attacks would cause the infected model's performance to

significantly drop, thus making the detection problem non-significant under our adversarial model (see Sec. 2). In practice, AP attacks could be rather threatening and easily implementable compared to backdoor attacks [17, 24, 33], due to (i) backdoor attacks typically exhibit the same shortcomings as evasion attacks [23, 29] where test-time instances are required to be modified, and (ii) technically, attackers could simply mislabel data during training to implement effective AP attacks [44].

Related Works on AP and Backdoor attacks. AP attack is considered to be a practical and easily implementable type of poisoning attacks in reality. AP attack requires fewer assumption regarding attacker's capability compared to backdoor attacks [42, 44] while preserving overall high accuracy on normal test-time inputs. Besides the common implementation of generating attacks through mislabeling training data [44], recent works on performing clean-label attacks which do not even require attackers to mislabel training data, including StingRay [44] and Poison Frog [42]. StingRay generates poisoned data which collides with adversarial images in the feature space, achieving > 99% attack success rate. Motivated by StingRay, Poison Frog [42] seeks to add perturbations containing features of the targeted infected label to yield poisoned data instances, which appear to be visually-indistinguishable from the corresponding original images. Poison Frog can achieve > 99% attack success rate under a more restricted attack model. The clean-label property clearly makes such AP attacks be more threatening in practice.

Regarding backdoor attacks, a recent set of attacks have been proposed, including BadNets [24], Trojan Attack [33], and Chen et al attack (denoted as "Chen Attack" throughout this paper) [17], which assume a stronger adversarial capability compared to AP attacks. BadNets [24] requires attackers to access the training dataset and inject poisoned data attached with arbitrary triggers. Trojan attack, which doesn't require attackers to access the training dataset, can achieve high attack success rate > 98% with fewer inserted poisoned instances. Chen attack, which is built under an adversarial model with weaker adversarial capability, injects random noise with certain transparency ratio as the backdoor trigger which overlaps with the entire image, can achieve > 99% attack success rate with a few poisoned data instances. Yao [52] proposes latent backdoor attack, which inserts a hidden trigger into a teacher model and this trigger can then be inherited by the student model through transfer learning, which does not apply to our attack model.

Existing detection methods against poisoning. A very recent set of works have been proposed to detect and mitigate backdoor attacks without accessing the original training dataset [31, 35, 49]. A fine-pruning method [31] was first proposed to remove backdoor by pruning neurons, which imposes trivial impact on prediction results given clean test inputs. Neural Cleanse [49], however, reports that this fine-pruning method may significantly reduce the classification accuracy on the GTSRB dataset. Neuron Trojan [35] presents three computation expensive methods to defend backdoor attacks, yet with rather limited evaluation only using the MNIST dataset. Note that both Fine-Pruning and Neuron Trojan focus on mitigation but not detection as they assume that a given model is already known to be poisoned.

Indeed, the problem of detecting poisoning attacks is significant and challenging. Trojan Attack [33] provides broad discussions on

several possible detection methods against backdoor attacks; yet Chen et al. [17] shows that a variety of these detection methods may fail in practice. To the best of our knowledge, Neural Cleanse [49] and ABS [32] represent the state-of-the-art detection and mitigation techniques which can effectively detect and mitigate certain backdoor attacks (i.e. BadNets and Trojan Attack) for image classification models.¹ Unfortunately, such detection methods exhibit limitations which may significantly constrain the applicability to more complex attack variants (e.g., they fail to detect multiple infected labels as shown in our evaluation) as well as AP attacks.

Regarding defenses against AP attacks, prior works mainly focus on sanitizing the poisoned training set and filtering poisoned samples [13, 28, 37, 40, 43]. However, such works are not applicable to our adversarial model (see Sec 3) where the detector shall not have access to the original training set which may contain poisoned instances. Under our more realistic adversarial model, unfortunately, there does not exist any detection and mitigation methods against AP attacks. As briefly discussed in [49], a fundamental challenge due to AP attacks is that different from backdoor attacks, AP attacks implement no unified rules (e.g., poisoned samples sharing the same trigger or common image properties on crating adversarial training data. Such unified rules are fundamentally observed and utilized in Neural Cleanse [49] and ABS [32], which perform a reverse engineering-based method which could identify the backdoor trigger. However, such observations do not hold for AP attacks because the poisoned training instances may not share any common feature. The poisoned training instances can be any images belonging to different classes and may not exhibit any feature in common (e.g., pixel, size, shape, etc.).

3 ADVERSARIAL MODEL

Attack Model. Our attack model is consistent with that of Neural Cleanse and ABS [32, 49]. Specifically, the attacker is assumed to fully control the DNN model, and be able to insert any type of poisoned data into the training dataset to achieve high attack success rate. A user may obtain a trained DNN model shared by a third party which exhibits state-of-the-art performance yet being infected by backdoor or AP attacks. Due to the fact that the poisoned data was used at the training phase, the user and the defender do not have access to such data. Any infected DNN model still performs generally well on clean test data yet exhibits targeted mis-classification when being tested with certain adversarial inputs, e.g., inputs of certain classes under adversarial poisoning or inputs being attached with a backdoor trigger, which guarantees the evasiveness of the vulnerabilities upon such infected models.

A DNN model is considered to be infected if misclassification is observed on any test inputs. In practice, there may exist multiple infected labels in a DNN model.

Defense Assumptions and Goals. We provide a detailed defender model against poisoning attacks, which is consistent with Neural Cleanse [49] and ABS [32] as well. The model consists of defining defender’s goal, defender’s knowledge and capability.

¹Note that there exist a couple of recent works on detecting backdoor attacks [16, 25], which are incrementally built upon Neural Cleanse, thus exhibiting same limitations and inabilities as Neural Cleanse in detecting backdoor and AP attacks. Also, insufficient evaluation is seen in the manuscripts.

Defender’s Goal. The defender has two specific goals. (i) **detecting vulnerabilities:** the defender needs to determine whether a given DNN model is infected by poisoning attacks, and more specifically, identify the infected labels, (ii) **mitigating vulnerabilities:** the defender needs to “clean” an infected model and remove any poisoning-induced vulnerabilities without affecting overall performance on clean test inputs.

Defender’s Knowledge and Capability. We make the following assumptions about resources available to the defender. We assume the defender has access to the trained DNN and clean datasets for detect purposes.² Also, the defender shall have access to sufficient computation resources to train or manipulate DNNs, e.g., GPUs or cloud services. However, the defender may not have access to the training configuration and the original training dataset which may contain poisoning instances. This is again because the model may be obtained through third-party sources and the original training process is thus totally a black box to both users and defenders. Moreover, if the DNN model is infected, the corresponding kind of poisoning technique shall be unknown to the defender.

4 DESIGN OF POISHYGIENE

4.1 Motivational Observations

Before presenting the detailed design, we first describe a set of interesting observations we obtain from extensive sets of experiments, which provide fundamental insights on designing PoisHygiene with ensured detection efficacy.

Observation 1: for an infected label, a poisoned decision region may co-exist with the healthy decision region. When using DNN models for classification problems, the concept of decision region refers to a specific region within the input space which corresponds to a unique output class and all points within this region contain one and only one output class [21].

Our first observation from extensive empirical studies reveals the existence of a poisoned decision region for any infected label (similar findings have also been discussed in [32, 49]). An infected label’s poisoned decision region may contain one output class different from the actual class, and may cover inputs belonging to other different classes. Note that such a poisoned decision region co-exists with the healthy decision region of an infected label, which preserves the overall high performance on normal test inputs under both AP and backdoor attacks.

Our empirical studies involve extensive implementation and evaluation using various state-of-the-art AP and backdoor attacks on multiple DNN models. Table 1 reports the attack success rate of implementing six existing poisoning techniques, including three AP attacks (i.e., StingRay [44], Poison Frog [42], and the common AP attack through mislabeling [44]—denoted as “Mislabel”) and three backdoor attacks [17, 24, 33] on a randomly-chosen label, for attacking the MNIST and GTSRB datasets. (Note that a complete set of evaluation results including other datasets are given in Table 8 in the appendix due to space constraints. For each dataset, we randomly generate (according to each tested attack technique) and use several

²Note that assuming access to clean datasets is common for works on detecting poisoning attacks, including Neural Cleanse, TAVOR, Neural Trojaning, ABS, Fine-Pruning [25, 31–33, 49]. It is a rather reasonable assumption as such clean datasets are often standardized and publicly available for various tasks (e.g., [2–6, 9, 11, 20].)

Conference'17, July 2017, Washington, DC, USA

Dataset	Attack Success Rate
MNIST(AP-Mislabel Attack)	99.4%
GTSRB(AP-Mislabel Attack)	96.5%
MNIST(AP-Poison Frog)	97%
GTSRB(AP-Pison Frog)	96%
MNIST(AP-StingRay)	97%
GTSRB(AP-StingRay)	96%
MNIST(BadNets)	100%
GTSRB(BadNets)	99.8%
MNIST(Trojan Attack)	99.4%
GTSRB(Trojan Attack)	97.2%
MNIST(Chen's)	100%
GTSRB(Chen's)	99.8%
MNIST(Healthy)-(AP)	2.9%
MNIST(Healthy)-(Backdoor)	0%
GTSRB(Healthy)-(AP)	0.1%
GTSRB(Healthy)-(Backdoor)	1.21%

Table 1: Attack efficacy using poisoned instances on both poisoned and healthy DNN models.

adversarial images as test inputs. We obtain the attack success rate using such test inputs for both infected and healthy DNN models, as reported in Table 1.

As seen in this table, for all infected models poisoned by the corresponding AP or backdoor technique, adversarial test inputs could cause the infected model to misclassify on a specific class with high attack success rate (close to 100%). Thus, it is highly likely that a poisoned region exists for the infected label in an infected model. Moreover, such a poisoned decision region is likely to be independent (not overlapping) from the healthy decision region for the infected label. This is because for healthy models, using a poisoned test input achieves a success rate of nearly 0, as seen in the last four rows of Table 1. This rate would have been noticeably higher if the healthy and poisoned decision regions overlap with each other.

The above observation motivates that it may be possible to design an effective detection method through accurately detecting whether a poisoned decision region exists for each label. To develop such detection methods, we further present the following two observations.

Observation 2: a poisoned decision region could be rather “vast”, not only corresponding to the poisoned instances seen in the infected training dataset, but could also be reached using other irrelevant test instances.

Previous works on designing backdoor attacks[17, 24, 33] have revealed the following interesting observation. For a backdoor-infected model, using images containing backdoor triggers as input could cause the model to misclassify on the infected class, even if the image is irrelevant to the training datasets. This may also apply to AP attacks, where inputs that are not seen in the training set can be misclassified as the infected label, possibly due to the strong generalization capability of neural networks [22]. We have also conducted extensive experiments which reveal the same observation. We list a couple of such instances for AP scenarios in Fig. 1. As shown in Fig. 1, the first column shows a poisoned sample from the training dataset, and the other four columns(from left to right) depict four images belonging to the same class yet not existing in the training dataset. Interesting, the images in the last four columns can yet be



Figure 1: Illustration on Observation 2 (AP scenario) using GTSRB and poisoned images containing McDonalds sign and airplanes. The first column shows a poisoned sample from the training dataset, and the other four columns (from left to right) depict four images belonging to the same class yet not existing in the training dataset.

misclassified as the infected label with high confidence(the number shown below each image in the figure) by the infected model. This implies the attack efficacy can still be ensured using inputs not existing in the training dataset. This observation also holds under backdoor scenarios, which is detailed in Figs. 9, 10 and 11 in the Appendix.

Observation 2 suggests that the poisoned decision region of an infected model could be rather vast, as for both AP and backdoor scenarios, it is not that difficult to craft inputs that would reach the poisoned decision region for an infected label. Even instances randomly crafted and not belonging to the original dataset may suffice. This encourages our intuition that it may be highly feasible to design detection methods that can smartly craft inputs to reach the poisoned decision region of an infected label.

Observation 3: for an infected label, its poisoned decision region could be “far away” from the healthy decision region belonging to the same label, where the distance could be indicated using the Cross Entropy Loss function which is widely used to measure the confidence of a prediction on a given pair of input and label. The above-discussed observations imply that for any infected model, a poisoned decision region may exist and could be reached using certain crafted inputs. Through conducting extensive experiments comparing the Cross Entropy Loss value computed on the poisoned input and its infected label under both a healthy and an infected version of the same model, we observe that, interestingly enough, the Cross Entropy Loss value under a healthy model is significantly larger than that under the infected model.

For AP attacks, we used the MNITS, Fashion-MNITS and GTSRB datasets. We randomly selected a label y_A as the infected label and trained a healthy state-of-art model T' using a clean dataset. We then retrain model T' using a poisoned dataset containing poisoned images to obtain an infected model T , which achieve a $\geq 99\%$ attack success rate following StingRay, Poison Frog, and Mislabel. In our experiments, we first randomly generate 1000 different inputs A collide with adversarial images in the feature space and ensure that these inputs would be classified as y_A by model T . We then calculate

Dataset	Loss value under Model T	Loss value under Model T'
MNIST(StingRay)	0.03	46.41
MNIST(Poison Frog)	0.1	39.26
MNIST(Mislabel)	0.12	43.56
Fashion-MNIST(StingRay)	0.12	43.21
Fashion-MNIST(Poison Frog)	0.11	41.21
Fashion-MNIST(Mislabel)	0.17	43.1
GTSRB(StingRay)	0.3	64.34
GTSRB(Poison Frog)	0.3	64.34
GTSRB(Mislabel)	0.09	64.34

Table 2: The Cross Entropy Loss value computed on the poisoned input and its infected label under a healthy and a corresponding infected model.

the corresponding Cross Entropy Loss value under both model T and T' for each of these 1000 inputs, and record the largest Loss value among all inputs, as shown in the Table. 2. We observe that the largest Loss value under the healthy model T' is very large (e.g., ≥ 41) while the Loss values under the infected model T are all close to 0. These results may imply that if a given model is infected, then the healthy decision region and the poisoned decision region could be “far away” from each other, as indicated by comparing the Cross Entropy Loss values. This is because a large Loss value under a healthy model implies that the input is “far away” from the healthy decision region belonging to the label; while a close to zero Loss value under the infected version of the same model implies that the same input is “close enough” to the poisoned decision region belonging to the same label.

The same observation holds for backdoor scenarios, as shown in Table 9 in the Appendix, where we similarly train a healthy and an infected version of a same model, following the three state-of-the-art backdoor attacks, BadNets [24], Trojan Attack [33], and Chen Attack [17].

Clearly, this observation motivates a key mechanism which may determine the existence of a poisoned decision region, through smartly crafting inputs, and calculating and evaluating the resulting Cross Entropy Loss values.

4.2 Detection Methodology

PoisHygiene is fundamentally motivated by the three observations discussed above. PoisHygiene aims to determine whether a given model T is infected by backdoor or AP attacks through determining for each label in T , whether a poisoned decision region exists. For each label y_t , PoisHygiene develops a method which smartly crafts an input instance x which could reach the poisoned decision region (if one exists) while being pushed away from the corresponding healthy decision region. This is done through manipulating the following optimization on the Cross Entropy Loss function as motivated by Observation 3:

$$x = \underset{x}{\operatorname{argmin}} \operatorname{Loss}_P(x, y_t) - \lambda * \operatorname{Loss}_N(x, y_t), \quad (1)$$

in which y_t represents the label to be analyzed, $\operatorname{Loss}_N(x, y_t)$ and $\operatorname{Loss}_P(x, y_t)$ represent the Loss function for measuring the classification error for the crafted input x under T 's the healthy and poisoned decision region (if any), respectively. Note that $\operatorname{Loss}(x, y_t)$ measures the error between a given label y_t and the predicted label on input x by a given model. A large $\operatorname{Loss}(x, y_t)$ thus may indicate a large prediction error.

Before presenting the intuition behind the above optimization procedure, we first have to answer an essential challenge in implementing this methodology. As seen in Eq. 1, an essential step of applying this optimization is to define and calculate Loss_N and Loss_P terms. First, due to the uninterpretability of DNNs, it is notoriously hard to understand the decision region corresponding to each label [21]. Also it is difficult (if not impossible) to identify or separate the healthy and poisoned decision regions in any concrete or quantifiable manner [21]. Thus, an essential challenge herein is that how to independently represent the healthy and poisoned decision region within the same given model T , which could enable calculating Loss_N and Loss_P in Eq. (1).

To address this challenge, instead of exploiting the healthy decision region in model T directly, we work on another model T_H , which inherits the structure of T entirely while being trained using clean training datasets.

Our intuition is that the healthy decision region of T_H would largely overlap with the healthy decision region of T for each label. This is intuitive since T_H and T share the same architecture, both of which can achieve state-of-the-art accuracy performance on a large amount of test data. We thus propose to use the healthy decision region of T_H to indicate that of T , thus being able to independently represent T_H 's healthy decision region and T 's poisoned decision region (if any).

Through utilizing model T_H , we propose to optimize the following objective:

$$x = \underset{x}{\operatorname{argmin}} \operatorname{Loss}_T(x, y_t) - \lambda * \operatorname{Loss}_{T_H}(x, y_t), \quad (2)$$

instead of directly optimizing Eq. 1. This alternative optimization suffices because optimizing $x = \underset{x}{\operatorname{argmin}} \operatorname{Loss}_T(x, y_t) - \lambda * \operatorname{Loss}_{T_H}(x, y_t)$ seeks to craft an x that is “far away” from the healthy decision region under T and T_H due to the second term in this equation, while ensuring to reach the poisoned decision region (if any) under T according to Observation 3 as discussed in Sec. 4.1. This implies exactly the same goal of optimizing Eq. 1.

The intuition behind Eq. (2) well matches with the Observation 3 presented in Sec. 4.1. Observation 3 essentially motivates the insight that if y_t is an infected label, then the corresponding poisoned decision region for y_t under T could be “far away” from the healthy decision region for y_t . The optimization function Eq. (2) has two objectives. For any (potentially infected) label y_t to be analyzed, the first objective is to lead the crafted input x into the poisoned decision region under T (if any) belonging to y_t . The second objective is to push x away from the healthy decision region belonging to y_t under T_H , thus that of T . Note that we introduce a co-efficient λ attached to the second objective to control the weight of each term in Eq. (2) and thus the optimization procedure. Thus, by optimizing Eq. 2, we aim at directing x into the poisoned decision region of T (if one exists) while being away from the corresponding healthy decision region.

Optimization procedure and detection criteria. The detailed optimization procedure including how to craft x as well as defining the detection criteria is shown in Algorithm 1, which contains three major steps. In the first step (Lines 4-5), we use gradient-descent to filter the crafted input x with a learning rate α as 0.01, which ensures x to be initialized beyond both poisoned and healthy decision regions for label y_t under model T . Forcing $\operatorname{Loss}_T(x, y_t) \geq 3$ shall indicate

Conference'17, July 2017, Washington, DC, USA

Algorithm 1 Pseudo-code for Optimizing Eq. 2

```

1: Input: random sample  $x$ , given label  $y_t$ 
2: Define:  $L1 = -Loss_T(x, y_t)$ 
3: Define:  $L2 = Loss_T(x, y_t) - \lambda * Loss_{T_H}(x, y_t)$ 
4: while  $Loss_T(x, y_t) <= 3$  do
5:    $x \leftarrow x - \alpha * \nabla_x L1(x)$ 
6: while  $i \leq MaxIters$  do
7:    $x \leftarrow x - \alpha * \nabla_x L2(x)$ 
8:   if  $Loss_T(x, y_t) <= \beta$  AND  $Loss_{T_H}(x, y_t) >= \gamma$  then
9:     BREAK
10: if  $Loss_T(x, y_t) <= \beta$  AND  $Loss_{T_H}(x, y_t) >= \gamma$  then
11:   Sample  $x$  reaches the poison decision region
12: else
13:   Sample  $x$  does not reach the poison decision region

```

that the crafted x is sufficiently far away from the poisoned decision region, because $Loss_T(x, y_t) \geq 3$ implies that the confidence of predicting x as y_t is smaller than 0.1. This constraint on crafting x is needed because for otherwise, x may easily (yet incorrectly) satisfy the detection criteria during early iterations of later optimization step (Lines 6-9). The second step (Lines 6-9) is simply a gradient-descent update which seeks to craft an x that minimizes Eq. 2 with a learning rate α . The third step (Lines 10-13) is used to identify whether the crafted sample x successfully reaches the poisoned decision region under T .

Importantly, Line 10 shows our detection criteria, where the first term $Loss_T(x, y_t) <= \beta$ indicates that x may be led into the poisoned decision region for y_t under model T ; while the second term $Loss_{T_H}(x, y_t) \geq \gamma$ implies that x is also sufficiently “far away” from the healthy decision region under model T_H (and thus under T as well), where $Loss_{T_H}(x, y_t)$ represents the cross entropy Loss value of input x with label y_t under model T_H . If a dominant portion of such inputs x meet the detection criteria for y_t , y_t is deemed to be an infected label. In the implementation, we set β to be 0.1 and γ to be 50% of the maximum value for which $Loss_{T_H}(x, y_t)$ can reach, motivated by extensive empirical evidence. Generally speaking, since the maximum value of $Loss_{T_H}(x, y_t)$ varies with model T_H for different tasks, we cannot simply adopt a constant value for γ . Instead, we adopt a variable associated with the maximum value of $Loss_{T_H}(x, y_t)$ for γ in our implementation.

Identify λ . To identify the best λ value for effectively identifying poisoned decision region, we propose to dynamically adjust λ to make $Loss_T(x, y_t) = \lambda \cdot Loss_{T_H}(x, y_t)$ hold after optimizing 1000 iterations of $(\arg \max_z Loss_T(z, y_t) + \lambda * Loss_{T_H}(z, y_t))$. Intuitively this is because through extensive empirical studies, we observe that the proper value of λ for identifying poisoned decision region varies depending on the specific pair of model T and T_H . Specifically, we observe that the detection efficacy gets maximized when during the procedure of crafting x , the value changing rates on $Loss_T(x, y_t)$ and $Loss_{T_H}(x, y_t)$ are kept roughly the same. We achieve such a balance through identifying λ which would enable $Loss_T(x, y_t)$ and $\lambda \cdot Loss_{T_H}(x, y_t)$ to increase roughly at the same rate during performing the optimization procedure

$(\arg \max_z Loss_T(z, y_t) + \lambda * Loss_{T_H}(z, y_t))$. This method of identifying a proper λ is also shown to be effective through extensive experiments.

4.3 Model-Ensemble: Enhancing Detection Efficiency and Scalability in Practice

For any given model T , we shall use the method presented in Sec. 4.2 to detect whether a poisoned decision region exists for T , thus determining whether T is infected. An essential step in PoisHygiene is to train a healthy model T_H inheriting T 's structure. In practice, it would be costly and inefficient to craft such a T_H given any T (considering the practical scenario where a model detection company may receive thousands of models from customers per day). To enable efficient and scalable detection service in practice, we propose the following model-ensemble approach.

Our idea on resolving this issue is the following: for each DNN-driven task (e.g., image classification), it may be possible to use a state-of-the-art model B to replace model T_H where both B and T perform the same task exhibiting state-of-the-art performance. Intuitively it may be possible because previous works have shown the transferability property of adversarial samples under healthy DNN models exhibiting completely different structures and parameters [38, 48].

To verify this idea, we perform a set of case studies using two datasets, MNIST and CIFAR-10. For each dataset, we randomly choose B from a pool of multiple state-of-the-art models listed in Tables 3 and 4 performing the corresponding tasks, yet forcing B and T to be different. As seen in Table 3, for MNIST,³ choosing any model in the pool as B under our approach can ensure a 100% true positive (TP) detection rate (i.e., any infected model will be detected as infected) and a 0% false positive rate (i.e., any healthy model will never be detected as infected). This results demonstrates that it is highly likely that the healthy decision region of models performing the same task may largely overlap with each other.

For the CIFAR-10 dataset, as seen in Table 4, while choosing any model in the pool as B can ensure an 100% true positive detection rate, it actually yields a rather high false positive rate simultaneously. The reason behind this observation is the following. For MNIST, the model pool contains straightforward convolution neural networks; while for CIFAR-10, the models in the pool are fairly complicated ones including RESNet and DenseNet, which may exhibit dramatic difference in structure, parameters, training data, and even different configurations for data augmentation. Therefore, there could be large variation in terms of the healthy decision region representation among these models. Such variation could diminish the overlapping portion of the healthy decision region between T and B . This could further cause the observation seen in Table 4, where PoisHygiene can still successfully detect any infected model T , yet may incorrectly deeming a healthy model T to be infected. This is because the non-overlapping region between the healthy decision region under B and T may be “far” away from B 's healthy decision region, as indicated by comparing the Cross Entropy Loss values. Thus,

³The models for MNIST are simply denoted as $B1, \dots, B5$ as they are straightforward convolution neural networks which yet achieve state-of-the-art performance due to the simplicity of this dataset.

model T_H	TP	FP
B1	100%	0%
B2	100%	0%
B3	100%	0%
B4	100%	0%
B5	100%	0%

Table 3: Results on MNIST task.

such regions have a higher possibility to be identified as a poisoned decision region under PoisHygiene.

For datasets that require complicated models which exhibit large variance, choosing a single model B to replace T_H may not be sufficient because the healthy decision region of B and T_H (thus that of B and T) may only partially overlap. The healthy decision region of B thus cannot accurately represent that of T . Any portion of the healthy decision region of T that is not overlapped with B 's healthy decision region would thus be deemed as the poisoned decision region under PoisHygiene, which would cause a healthy model to be detected as infected (i.e., a high false positive detection ratio as seen in the CIFAR-10 case study).

To resolve this challenge, we patch an enhancement method to PoisHygiene, namely model-ensemble. The key idea behind this approach is that instead of using a single model to replace T_H , PoisHygiene would use a model ensemble B which contains a pool of models performing the same task as the given model T . The benefit is intuitive: using multiple models to replace T_H would increase the overlapping degree between the healthy decision region of T and the joint healthy decision region of all models in this model ensemble. Specifically, B would be a model ensemble, consisting of a set of models. Thus, we could accordingly update Eq. 2 using the following Eq. 3 during the detection procedure:

$$x = \underset{x}{\operatorname{argmin}} \operatorname{Loss}_T(x, y_t) - \sum_{i=1}^k \lambda_i * \operatorname{Loss}_{B_i}(x, y_t), \quad (3)$$

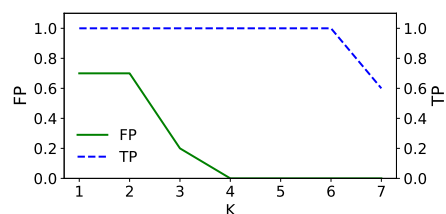
where k represents the number of models in the model ensemble, B_i denotes a model belonging to this ensemble, and λ_i denotes the co-efficient for each B_i .

For the same CIFAR-10 case study, Fig.2 shows the results on the false positive detection rate if applying this model ensemble approach. As seen in this figure, a larger value of k would effectively reduce the false positive detection rate. A model ensemble B containing at least 4 models would reduce the false positive rate to 0. (More extensive experiments to be described in Sec. 5.2 also prove the efficacy of this model-ensemble approach.)

5 EXPERIMENTAL VALIDATION

In this section, we describe experiments conducted to assess the efficacy of PoisHygiene against state-of-the-art AP and backdoor attacks under various datasets and system settings. Our evaluation focuses on answering the following key research questions: (i) can PoisHygiene achieve high overall detection rate? (ii) can PoisHygiene enhance the detection performance when comparing to state-of-the-art detection methods? (iii) is PoisHygiene sufficiently robust considering different settings and attack variants?

model T_H	TP	FP
RESNet.V1.44	100%	70%
RESNet.V2.102	100%	80%
DenseNet-121	100%	80%
DenseNet-40	100%	80%
RESNet.V2.83	100%	70%

Table 4: Results on CIFAR-10 task.

Figure 2: FP and TP with different k

5.1 Experiment Setup

Datasets and models. We evaluated PoisHygiene upon five datasets using a set of state-of-the-art DNN models, including (1) MNIST for the hand-written digit recognition task, (2) Fashion-MNIST for the fashion item recognition task, (3) GTSRB for the traffic sign recognition task, (4) CIFAR-10 for the image classification task, and (5) YouTube Face for the large scale face recognition task. Due to space constraints, we detail each dataset/task, as well as training configuration and model architecture and parameters in the Appendix.

Attack Configuration for AP. We evaluated two dominate types of integrity AP attacks [42, 44]: (i) clean-label AP attack implemented as Poison Frog [42] and Sting Ray [44], and (ii) integrity poisoning attack using mislabeled data implemented as the attack described in [44] (denoted “Mislabel”). Our attack configurations exactly follow the configuration described in the corresponding papers [42, 44].

For each task, we select at random a label as the infected label and choose images of a certain class as poisoned inputs(details are shown in Table. 10 in the Appendix). To measure attack performance, we calculate classification accuracy on the test data, as well as the attack success rate when using adversarial images as test inputs. The Attack Success Rate metric measures the percentage of adversarial inputs being mis-classified as the infected label. We also measure the classification accuracy on a clean version of each model (i.e. training using exactly the same configuration but with clean training set- T_H corresponding to each given T) For each dataset and task, we vary the proportion of poisoned inputs(from 4% to 8%) to ensure a $\geq 94\%$ attack success rate while preserving overall classification performance.

Attack Configuration for Backdoor. We evaluated three state-of-the-art backdoor attack methods including BadNets, Trojan Attack and Chen Attack [17, 24, 33], which represent the state-of-the-art as well as the only existing backdoor attack techniques that are effective under our adversarial model. The attack configuration and trigger selection in the evaluation are consistent with the setting adopted by Neural Cleanse [49], which focuses on detecting backdoor due to BadNets and Trojan Attack. For Chen attack, we set the random noise based trigger to occupy the entire image and set a transparency ratio of 0.1 to make the trigger appear less noticeable.

Example poisoned images and triggers are shown in Fig. 12 in the Appendix. As seen in Table 11 in the appendix, our chosen attack configuration ensures that all tested backdoor attacks achieve $\geq 97\%$ attack success rate, with trivial impact on overall classification accuracy.

Evaluation Metrics. Prob—To imply the detection efficacy for each label y_t , we use the proportion of those x among all crafted ones which satisfy the detection criteria for reaching the poisoned decision region as discussed in Sec 4.2 (denoted as Prob). Specifically, a

Conference'17, July 2017, Washington, DC, USA

Dataset	StingRay	Poison Attack	Mislabel Attack	BadNets	Trojan Attack	Chen attack
MNIST	98%(0%)	98%(0%)	100%(0%)	100%(0%)	100%(0%)	100%(0%)
Fashion-MNIST	86%(0%)	86%(0%)	86%(0%)	89%(0%)	89%(0%)	86%(0%)
GTSRB	83%(0%)	83%(0%)	86%(0%)	96%(0%)	83%(0%)	90%(0%)
CIFAR-10	100%(40%)	100%(40%)	100%(40%)	100%(40%)	100%(40%)	100%(40%)
YoutubeFace	85%(0%)	85%(0%)	89%(0%)	100%(0%)	100%(0%)	100%(0%)

Table 5: Prob value on the infected label and FP rate on various datasets leveraging T_H

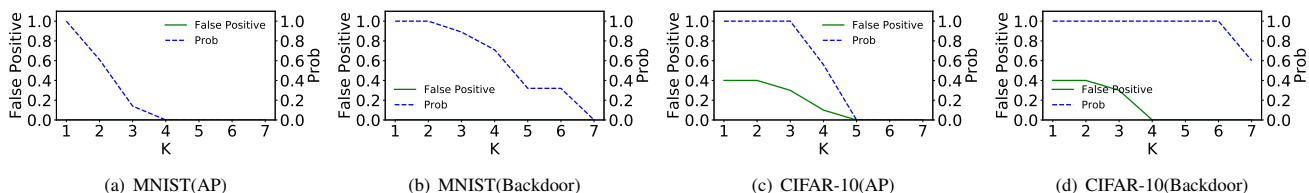


Figure 3: Prob value and FP rate with different k for MNIST and CIFAR-10 under backdoor and AP attacks scenarios.

Prob value larger than 50% would indicate that a given label y_t is an infected label. Note that using Prob as a metric can indicate detection performance while showing in detail the number of crafted x under Poishygiene that are effective towards detection purpose.

False positive rate—For any detection method to be effective in practice, besides detection rate, yielding a low false positive (FP) rate is equally important. A zero or close-to-zero FP rate would indicate that the detection method under evaluation would prevent mis-tagging any clean labels.

For each experiment on each dataset, we randomly selected a model from the corresponding model pool and repeated this process for ten times. We then create two model sets based upon these ten selected models, including an infected set where we infect each of these ten models following each evaluated attack method, as well as a healthy set where all ten models are healthy. The infected set is used to evaluate the Prob metric (thus the detection efficacy). It is also used for measuring the FP rate, as any infected model may contain clean labels as well. The healthy set is used to evaluate the FP rate under Poishygiene. We crafted 100 samples (i.e., x) for each experiment. We note that when implementing the model ensemble method, we intentionally remove the model from the ensemble which exhibits the same architecture as the model to be analyzed.

5.2 Overall Detection Performance

In this section, we perform experiments to evaluate Poishygiene following the methodology in Secs. 4.2 and 4.3, i.e., using T_H and a model-ensemble for detection purpose, respectively. Moreover, for backdoor scenarios, we compare performance of Poishygiene to Neural Cleanse [49] and ABS under various settings.⁴

Performance using T_H . Table 5 shows the minimum Prob among all ten infected models in each experiment and the FP rate for all the six implemented attacks. As seen in Table. 5, for each attack method, the Prob of the infected label is higher than 50%, indicating

⁴Note that we choose to compare against Neural Cleanse and ABS because they represent state-of-the-art methods on detecting backdoor attacks. We are also aware of a couple of other works on detecting backdoor attacks [16, 25], which are too premature (i.e., with no or very limited evaluation) and incrementally built upon Neural Cleanse to be included in the comparison. Also note that there does not exist any detection method on the AP attacks evaluated in this paper.

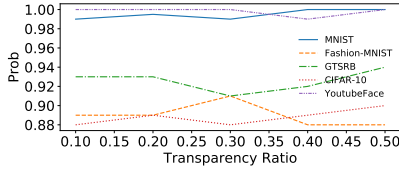
Poishygiene is effective in detecting the infected label. Meanwhile, following each attack methodology, for all datasets except CIFAR-10, Poishygiene yields a zero FP rate. The high FP rate for CIFAR-10 is caused by the inability of using a single T_H to deal with such complex datasets, as discussed in Sec 4.3.

Performance using the Model Ensemble. As discussed in Sec. 4.3, Poishygiene also contains a model ensemble method to enhance its efficiency and scalability in practice. For evaluation, we create a model pool containing a set of state-of-the-art DNN models for each tested dataset. For each experiment, we randomly choose a model in the pool as the model to be detected, and treat the remaining models as the model ensemble. We note that in order to ensure practicality and robustness of this approach, the models contained inside each model pool may exhibit dramatically different structures and parameters (e.g., DenseNet versus RESNet). Detailed model information is described in the Appendix.

We first seek to understand how k , the number of models used in the model ensemble, would impact the performance w.r.t. both Prob on infected label and FP rates. Results in terms of minimum Prob are shown in Fig. 3 (results on the remaining datasets are put in Fig. 13 in the Appendix. As seen in Figs. 3 and 13, we observe that for relatively simple datasets including MNIST, Fashion-MNIST and GTSRB, a small k value (e.g., $k \leq 2$) would be sufficient in ensuring $Prob \geq 50\%$ and an FP rate close to 0. Thus, for rather simple datasets where using plain convolution networks is sufficient to obtain state-of-art performance, a model ensemble containing one or two models would be sufficient to guarantee detection performance.

On the other hand, for more complex datasets such as CIFAR-10 and YoutubeFace, only a sufficiently large k (e.g., $k \geq 4$) could result in a low FP rate $\leq 21\%$. This is again because using a model ensemble may ensure a large overlapping between the healthy decision region of T and the models in the ensemble B , as discussed in Sec 4.3. Another observation is that a too large k value (e.g., $k \geq 5$) would cause the Prob value to be dropped under 0.5, which implies a low detection rate. This is because when the model ensemble B contains too many models, the resulting entire healthy decision region of models in B may become rather vast, increasing the possibility of covering cover regions that are close to the poisoned decision region under T . Thus, a preferred k value for CIFAR-10 and YoutubeFace

Prob(FP Rate) \ Attack Technique	StingRay	Poison Frog	Mislabel Attack	BadNets	Trojan Attack	Chen et al
Dataset						
MNIST	98%(0%)	98%(0%)	100%(0%)	100%(0%)	100%(0%)	100%(0%)
Fashion-MNIST	86%(0%)	86%(0%)	86%(0%)	89%(0%)	89%(0%)	86%(0%)
GTSRB	83%(0%)	83%(0%)	86%(0%)	96%(0%)	83%(0%)	90%(0%)
CIFAR-10	51%(10%)	51%(10%)	56%(10%)	100%(10%)	100%(10%)	100%(10%)
YoutubeFace	100%(21%)	100%(21%)	100%(21%)	100%(21%)	100%(21%)	100%(21%)

Table 6: Prob value on the infected label and FP rate on various datasets leveraging a model ensemble B

Figure 4: Detection Performance under different transparency ratio of noise in each task for Chen Attack under PoisHygiene.

datasets is set to be four, which is able to achieve a sufficiently large Prob value and a low FP rate.

Table. 6 shows the performance of PoisHygiene for the evaluated datasets and attack methods under the model ensemble approach with an appropriate k value set for each dataset, as discussed above. As seen in the Table, PoisHygiene is able to achieve sufficiently good Prob values (100% under most settings) while ensuring low FP rates (0% under most settings).

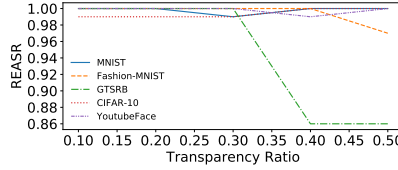
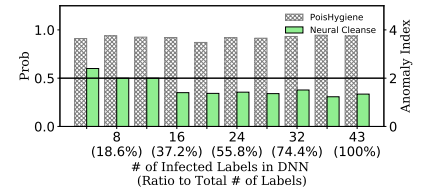
5.3 Performance on BD attacks compared to Neural Cleanse and ABS

We specifically compared PoisHygiene using the model ensemble approach against Neural Cleanse and ABS on detecting backdoor attacks under various complex attack variants.

Performance against advanced backdoor attack, i.e., Chen Attack [17]. For more advanced backdoor attack methods, we compare PoisHygiene to Neural Cleanse and ABS [32] for detecting models infected by Chen Attack, which applies a semi-transparent random noise to the entire input. As seen in Fig. 4, PoisHygiene is able to yield a $Prob \geq 50\%$, which implies a perfect detection under all transparency settings; while Neural Cleanse simply fails to detect any infected label under all tested scenarios. As discussed earlier, Neural Cleanse cannot handle such backdoor attacks which do not constraint the trigger size. We also test PoisHygiene against ABS on Chen attack with the same settings. As shown in Fig. 5, ABS can also successfully detect the infected label correctly with the attack success rate indicated by the reverse engineered trojan trigger (REASR) higher than 80% on various datasets.

Multi-Label Detection. We also evaluated the scenario where multiple infected labels are present in the given model. We follow the configuration as previous experiments, with the only exception of omitting the evaluation on YoutubeFace. This is because multiple infected labels would cause the overall accuracy to significantly drop on YoutubeFace [49].

Note that for PoisHygiene, we select the minimum Prob value among all infected labels to represent the Prob value under each tested model. As seen in the Fig. 6, PoisHygiene can achieve a


Figure 5: Detection Performance under different transparency ratio of noise in each task for Chen Attack under ABS.

Figure 6: Multi-Label Detection Performance on GTSRB compared to Neural Cleanse

significantly higher detection rate than Neural Cleanse with multiple (≥ 12) infected labels under GTSRB, while achieving zero FP rate. (Again, results on other datasets are put in the Fig. 14 in the Appendix. In fact, when the model contains ≥ 12 infected labels, Neural Cleanse fails to detect any such label. This is because Neural Cleanse applies an outlier method. (Note that the detection criteria on infected labels under Neural Cleanse is: anomaly index ≥ 2). ABS suffers from the same issue as its design and evaluation only focus on the single infected label case.

Being able to detect multi-infected-label models is critical as in practice, attackers may very likely create multiple infected labels to prevent the infected model from being detected.

6 MITIGATION OF ATTACKS

After successfully identifying the infected label, we now show how to implement our proposed unlearning-based mitigation technique while maintaining the overall performance.

6.1 Mitigation via Unlearning

Our proposed mitigation method is to train the infected models to unlearn adversarial images. For each label y_o , where y_o denotes the label other than infected label y_t , we craft several adversarial images by optimizing Eq. 4 given below, and then use pairs of the crafted adversarial image and its corresponding label y_o to retrain the infected DNN.

To perform the unlearning process, we first need to identify several adversarial images used in the process. We craft adversarial images by optimizing the following objective:

$$x = \underset{x}{\operatorname{argmin}} \operatorname{Loss}_T(x, y_t) + c * \operatorname{Loss}_{T_H}(x, y_o) - d * \operatorname{Loss}_{T_H}(x, y_t), \quad (4)$$

Recall that the goal of optimizing Eq. 2 is to craft an input that would reach the poisoned decision region under model T . Thus, optimizing Eq. 4 enables us to obtain an adversarial image that could simultaneously reach poisoned decision region of y_t under model T and the healthy decision region of y_o under model T_H . To ensure that the crafted adversarial images could reach the poisoned decision region of y_t under T and the healthy decision region of

Conference'17, July 2017, Washington, DC, USA
 y_o under T_H , we adjust c and d properly to ensure that $Loss_T(x, y_t)$ and $Loss_{T_H}(x, y_o)$ both being smaller than 0.01. After obtaining adversarial images, we can then patch via unlearning for mitigation.

6.2 Mitigation Performance including Comparison to Neural Cleanse

In our experiments on evaluating mitigation performance, for each infected model, we retrain the infected model for five iterations with a mixed dataset. To create this mixed dataset, we take 10% samples of the original healthy training data and add crafted adversarial samples which count for 20% of these healthy data. Note that for each crafted adversarial sample, we label it using the corresponding infected label y_o , and label all other healthy samples using the correct labels. We use the attack success rate due to the original trigger and classification accuracy after applying our unlearning-based mitigation process as the metric to measure the mitigation performance. We compare our method against the unlearning-based mitigation method proposed in Neural Cleanse which represents the only existing method which can patch DNNs infected by backdoor attacks under a practical adversarial model.

The results are shown in Table 7. Columns 2-5 of this table show the attack success rate and classification accuracy before and after applying our mitigation approach. As seen in the table, for each task, our approach manages to reduce the attack success rate to be below 6.1%, without noticeably reducing the overall performance (i.e., the largest seen accuracy reduction is only 3.92% on Fashion-MNIST infected by Chen Attack).

Next, we compare PoisHygiene with Neural Cleanse (Columns 6-7). We observe that both two approaches are sufficiently effective for mitigating backdoor attacks due to BadNets and Trojan attack. However, similar to detection, under Chen attack and all types of AP attacks, Neural Cleanse cannot identify the infected label and thus fails in the mitigation phase; while PoisHygiene can mitigate these attacks and reduce the attack success rate to be $< 7.7\%$ under all scenarios.

Finally, we compare against unlearning using only clean training data (no additional triggers), as shown in Columns 8-9 in Table 7. We observe that unlearning using only clean data is ineffective for all tasks under both BadNets and AP attacks (i.e., still yielding a high attack success rate $\geq 95.46\%$ for BadNets and $\geq 79\%$ for AP attacks). Nonetheless, unlearning using only clean training data remains effective for models affected by Chen Attack and Trojan Attack, with attack success rates being reduced from 13% to 7.18%. This may be due to the fact that Chen Attack and Trojan attack are much more sensitive to training only using clean data. Such clean data may reset certain parameters of the infected model, thus disabling the attack. In contrast, BadNets and AP attacks seem to be insensitive to unlearning using clean training data, which nonetheless can be effectively mitigated by PoisHygiene.

7 ROBUSTNESS UNDER OTHER ATTACK VARIANTS

For evaluating the robustness of PoisHygiene, we have conducted a set of experiments considering various attack variants (note that several such variants, e.g., multi-label detection, have been evaluated in Sec. 5).

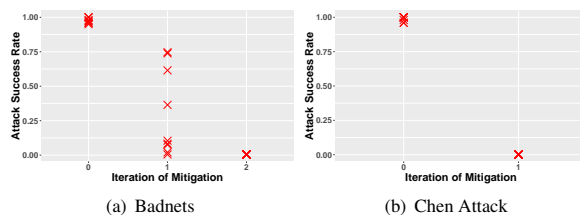


Figure 7: Attack Success Rate and Prob when mitigating models with multiple iterations under BadNets and Chen Attack.

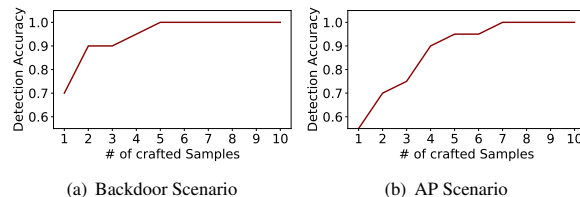


Figure 8: Impact due to the number of crafted x

Single Infected Label due to Multiple Triggers. We also evaluated scenarios where the attacker may apply multiple triggers for infecting a single label. The tested setup is that we apply nine different triggers in the form of either 4x4 white square (BadNets) or random noise with a 0.1 transparency ratio and different patterns (Chen Attack), located at different locations in an image, which yields a $\geq 95\%$ attack success ratio.

The mitigation results are shown in Fig. 7(a),7(b). We observe that with multiple triggers, a single run of our detection and mitigation can only patch a partial set of triggers. Interestingly, after the first run, the Prob of the infected label is still higher than 0.5 as shown in Fig. 7(a), which indicates there may be some remaining triggers. Therefore, we could simply run multiple iterations and successfully mitigate all triggers, i.e., reducing the attack success rate and Prob to nearly zero.

Interestingly, under Chen Attack implementing random noise-based trigger, running PoisHygiene just once could actually patch all patterns as shown in Fig. 7(b). We also test on other datasets including GTSRB, Fashion-MNIST, and CIFAR-10, and the attack success rate for all triggers could be reduced to nearly 5.19%, 0.79%, 5.72% after running 2-4 iterations. This may be again due to the fact that Chen Attack is sensitive to clean training data as discussed in 6.

Impact due to single-trigger implementation. In prior experiments, we have tested our approach under the scenario where multiple triggers are located at different positions for each infected label. In this experiment set, we test the setting where only one trigger is used but placed at different locations for each infected label on various datasets. The results are similar to Table. 6, which demonstrate that PoisHygiene is resilient to different trigger locations. We also test the setting where complicated trigger patterns (e.g., in terms of trigger shape) are implemented. The results on Trojan and Chen attacks prove the efficacy, as detailed in Table. 19 in the Appendix.

Impact due to the Number of the crafted x . Our detection method has been proved effective through extensive experiments under the setting where 100 crafted samples (i.e., x) are generated for each detection task. Intuitively, generating more random samples could

Task	Before Unlearning		After applying PoisHygiene		After applying Neural Cleanse		Unlearning using Clean Data	
	Classification Accuracy	Attack Success Rate	Classification Accuracy	Attack Success Rate	Classification Accuracy	Attack Success Rate	Classification Accuracy	Attack Success Rate
MNIST(BadNets)	98.26%	99.99%	97.24%	0.42%	97.49%	0.59%	97.84%	95.21%
GTSRB(BadNets)	96.79%	100%	93.26%	4.15%	92.91%	0.14%	93.43%	96.16%
Fashion-MNIST(BadNets)	90.93%	100%	87.94%	0.93%	88.01%	0.44%	88.61%	95.46%
CIFAR-10(BadNets)	93.26%	97.14%	90.28%	5.12%	90.17	4.14%	89.44%	93.34%
YoutubeFace(BadNets)	97%	97.5%	97.7%	7.12%	97.9	6.7%	97.8%	95.4%
MNIST(Trojan)	97.34%	99%	97.13%	0.12%	97.49%	0.59%	97.84%	10.6%
Fashion-MNIST(Trojan)	90.16%	97%	87.94%	0.9%	88.01%	0.64%	88.61%	10.6%
GTSRB(Trojan)	96.32%	97.61%	94.07%	1.28%	94.61%	1.07%	96.43%	9.26%
CIFAR-10(Trojan)	90.21%	98.26%	91.28%	2.17%	90.17	5.13%	89.44%	7.18%
YoutubeFace(Trojan)	95.21%	99%	96.1%	5.14%	97%	4.9%	97%	8.31%
MNIST(Chen et al)	98.47%	100%	97.24%	0.51%	N/A	N/A	97.89%	11%
Fashion-MNIST(Chen et al)	90.49%	98.43%	88.01%	2.51%	N/A	N/A	88.68%	13%
GTSRB(Chen et al)	96.64%	100%	92.71%	6.1%	N/A	N/A	94.17%	10.93%
CIFAR-10(Chen et al)	90.39%	98.31%	88.41%	4.35%	N/A	N/A	89.26%	13.2%
YoutubeFace(Chen et al)	97.2%	97.5%	97.7%	6.7%	N/A	N/A	97.8%	11%
MNIST(Mislabel)	99.11%	100%	97.89%	0.13%	N/A	N/A	97.87%	89.31%
Fashion-MNIST(Mislabel)	92.9%	98.1%	90.06%	1.06%	N/A	N/A	91.47%	79.21%
GTSRB(Mislabel)	96.31%	95.72%	93.19%	5.3%	N/A	N/A	93.48%	81.5%
CIFAR-10(Mislabel)	91.29%	97.06%	85.81%	7.64%	N/A	N/A	90.07%	81%
YoutubeFace(Mislabel)	99.13%	97.81%	95.21%	0%	N/A	N/A	99.13%	83.51%
MNIST(Poison Frog)	98.71%	98.28%	97.61%	0.17%	N/A	N/A	97.85%	88.62%
Fashion-MNIST(Poison Frog)	91.23%	98.1%	89.72%	1.06%	N/A	N/A	91.47%	79.18%
GTSRB(Poison Frog)	96.31%	95.69%	93.19%	5.3%	N/A	N/A	94%	81.5%
CIFAR-10(Poison Frog)	90.97%	97.06%	87.11%	7.62%	N/A	N/A	89.44%	81.18%
YoutubeFace(Poison Frog)	97.66%	98.91%	95.82%	0%	N/A	N/A	98.91%	83.51%
MNIST(StingRay)	99.01%	98.2%	98%	0.17%	N/A	N/A	99.01%	88.62%
Fashion-MNIST(StingRay)	92.83%	98.1%	90.09%	2.07%	N/A	N/A	92.01%	80.61%
GTSRB(StingRay)	97.1%	95.16%	96.48%	5.23%	N/A	N/A	97.1%	81.5%
CIFAR-10(StingRay)	92.67%	98.1%	88.51%	7.21%	N/A	N/A	90.03%	83.2%
YoutubeFace(StingRay)	97.81%	98.91%	95.41%	0%	N/A	N/A	97.81%	82.18%

Table 7: Mitigation performance.

ensure better detection accuracy. To investigate the impact on detection performance due to the number of crafted samples, we evaluate PoisHygiene again on GTSRB under both backdoor and AP scenarios. For backdoor attack (BadNets), we implement a 4x4 white square trigger; for AP attacks, we implement Poison Frog.

The results averaged over 100 runs are shown in Fig. 8, where the x-axis represents the number of crafted samples, and the y-axis represents the resulting detection accuracy, where detection accuracy denotes the proportion of the runs in which both the infected model and the corresponding specific infected label are correctly detected among 100 runs. We observe that the detection accuracy increases with an increasing number of random samples under both scenarios. Surprisingly, for detecting backdoor, PoisHygiene can ensure 100% detection accuracy using just five crafted samples; while under AP attack scenario, seven crafted samples could already ensure detection efficacy. We have also tested on MNIST, Fashion-MNIST, CIFAR-10, and YoutubeFace, showing that the minimum number of crafted samples which could ensure detection efficacy ranges from four to ten under different attack techniques. Thus, crafting ten samples is sufficient to ensure successful detection in most cases, which could yield a significantly reduced computation overhead in practice.

Unawareness of the original training dataset. In previous experiments, we use publicly-available training datasets (e.g., MNIST, GTSRB) as clean datasets to create model T_H , which may also be used by the given model T to be analyzed. Since it is impractical for the defender to access the original training dataset used for training T , we consider herein the scenario where the clean portion of the datasets used by the attacker and defender are partially or completely

different. In this set of experiments, we create an infected model and five clean models on CIFAR-10 following the configuration of previous experiments. These models all exhibit different structures and parameters, and the clean training data for each model uses different data augmentation configuration, indicating that the clean portion of the training datasets used for training T and models in the model ensemble are at least partially different. We use the five clean models to analyze the infected model under our model ensemble approach for the complex CIFAR-10 dataset. The results are the same as previous experiments where same clean training datasets are used to train these models, yielding a 100% Prob and a 0% FP rate.

We also test on MNIST, where we divide the original cleaning training dataset contains 60000 images equally into 3 subsets, and create two models with different architectures trained using two of the three subsets. Note that these three subsets are completely different. These two models can achieve a $\geq 98.8\%$ classification accuracy. We then use the third subset plus poisoned data to train an infected model, and analyze the infected model using the two clean models as T_H under PoisHygiene. The obtained results are also the same as the earlier-described experiments performed on MNIST. This demonstrates that PoisHygiene is still effective when the defender is totally unaware of the original training data used to train a given model T .

8 CONCLUSION

In this paper, we present PoisHygiene, a practical and robust technique for detecting and mitigating backdoor and AP attacks on

Conference'17, July 2017, Washington, DC, USA
 neural networks. Extensive evaluation proves the efficacy and robustness of PoisHygiene under various settings considering complex attack variants. Such efficacy is also demonstrated through comparison against a state-of-the-art backdoor detection and mitigation technique.

REFERENCES

- [1] 1911. Nobel prize. <https://www.nobelprize.org/prizes/chemistry/1908/rutherford/biographical/>. (1911).
- [2] 1998. MNIST. <http://yann.lecun.com/exdb/mnist/>. (1998).
- [3] 2009. CIFAR. <https://www.cs.toronto.edu/~kriz/cifar.html>. (2009).
- [4] 2010. ImageNet. <http://www.image-net.org/>. (2010).
- [5] 2011. German Traffic sign. <http://benchmark.ini.rub.de/?section=gtsrb&subsection=news>. (2011).
- [6] 2011. YoutubeFace. <https://www.cs.tau.ac.il/~wolf/ytfaces/>. (2011).
- [7] 2017. Gradient ZOO. <https://www.gradientzoo.com/>. (2017).
- [8] 2017. Model ZOO. <https://modelzoo.co>. (2017).
- [9] 2017. Public Face. <http://www.face-rec.org/databases/>. (2017).
- [10] 2017. Pytorch ZOO. <https://pytorch.org/hub>. (2017).
- [11] 2018. CASIAN. <https://www.kaggle.com/sophatvathana/casia-dataset>. (2018).
- [12] James Cannady. 1998. Artificial neural networks for misuse detection. In *National information systems security conference*, Vol. 26. Baltimore.
- [13] Yinzi Cao, Alexander Fangxiao Yu, Andrew Aday, Eric Stahl, Jon Merwine, and Junfeng Yang. 2018. Efficient repair of polluted machine learning systems via causal unlearning. In *Proceedings of the 2018 Asia Conference on Computer and Communications Security*. ACM, 735–747.
- [14] Bryant Chen, Wilka Carvalho, Nathalie Baracaldo, Heiko Ludwig, Benjamin Edwards, Taesung Lee, Ian Molloy, and Biplav Srivastava. 2018. Detecting backdoor attacks on deep neural networks by activation clustering. *arXiv preprint arXiv:1811.03728* (2018).
- [15] Chenyi Chen, Ari Seff, Alain Kornhauser, and Jianxiong Xiao. 2015. Deepdriving: Learning affordance for direct perception in autonomous driving. In *Proceedings of the IEEE International Conference on Computer Vision*. 2722–2730.
- [16] Huili Chen, Cheng Fu, Jishen Zhao, and Farinaz Koushanfar. 2019. Deepinspect: A black-box trojan detection and mitigation framework for deep neural networks. In *Proceedings of the 28th International Joint Conference on Artificial Intelligence*. AAAI Press, 4658–4664.
- [17] Xinyun Chen, Chang Liu, Bo Li, Kimberly Lu, and Dawn Song. 2017. Targeted backdoor attacks on deep learning systems using data poisoning. *arXiv preprint arXiv:1712.05526* (2017).
- [18] Zheng Leong Chua, Shiqi Shen, Prateek Saxena, and Zhenkai Liang. 2017. Neural nets can learn function type signatures from binaries. In *26th {USENIX} Security Symposium ({USENIX} Security 17)*, 99–116.
- [19] Joseph Clements and Yingjie Lao. 2018. Hardware trojan attacks on neural networks. *arXiv preprint arXiv:1806.05768* (2018).
- [20] Fashion-MNIST. 2017. Fashion-MNIST. <https://github.com/zalando-research/fashion-mnist>. (2017).
- [21] Alhussein Fawzi, Seyed-Mohsen Moosavi-Dezfooli, Pascal Frossard, and Stefano Soatto. 2017. Classification regions of deep neural networks. *arXiv preprint arXiv:1705.09552* (2017).
- [22] Robert Geirhos, Carlos RM Temme, Jonas Rauber, Heiko H Schütt, Matthias Bethge, and Felix A Wichmann. 2018. Generalisation in humans and deep neural networks. In *Advances in Neural Information Processing Systems*. 7538–7550.
- [23] Ian J Goodfellow, Jonathon Shlens, and Christian Szegedy. 2014. Explaining and harnessing adversarial examples. *arXiv preprint arXiv:1412.6572* (2014).
- [24] Tianyu Gu, Brendan Dolan-Gavitt, and Siddharth Garg. 2017. Badnets: Identifying vulnerabilities in the machine learning model supply chain. *arXiv preprint arXiv:1708.06733* (2017).
- [25] Wenbo Guo, Lun Wang, Xinyu Xing, Min Du, and Dawn Song. 2019. TABOR: A Highly Accurate Approach to Inspecting and Restoring Trojan Backdoors in AI Systems. *arXiv preprint arXiv:1908.01763* (2019).
- [26] Kaiming He, Xiangyu Zhang, Shaoqing Ren, and Jian Sun. 2016. Deep residual learning for image recognition. In *Proceedings of the IEEE conference on computer vision and pattern recognition*. 770–778.
- [27] Gao Huang, Zhuang Liu, Laurens Van Der Maaten, and Kilian Q Weinberger. 2017. Densely connected convolutional networks. In *Proceedings of the IEEE conference on computer vision and pattern recognition*. 4700–4708.
- [28] Matthew Jagielski, Alina Oprea, Battista Biggio, Chang Liu, Cristina Nita-Rotaru, and Bo Li. 2018. Manipulating machine learning: Poisoning attacks and countermeasures for regression learning. In *2018 IEEE Symposium on Security and Privacy (SP)*. IEEE, 19–35.
- [29] Yujie Ji, Xinyang Zhang, Shouling Ji, Xiapu Luo, and Ting Wang. 2018. Model-reuse attacks on deep learning systems. In *Proceedings of the 2018 ACM SIGSAC Conference on Computer and Communications Security*. ACM, 349–363.
- [30] Yann LeCun, Yoshua Bengio, et al. 1995. Convolutional networks for images, speech, and time series. *The handbook of brain theory and neural networks* 3361, 10 (1995), 1995.
- [31] Kang Liu, Brendan Dolan-Gavitt, and Siddharth Garg. 2018. Fine-pruning: Defending against backdooring attacks on deep neural networks. In *International Symposium on Research in Attacks, Intrusions, and Defenses*. Springer, 273–294.
- [32] Yingqi Liu, Wen-Chuan Lee, Guan hong Tao, Shiqing Ma, Yousra Aafer, and Xiangyu Zhang. 2019. ABS: Scanning neural networks for back-doors by artificial brain stimulation. In *Proceedings of the 2019 ACM SIGSAC Conference on Computer and Communications Security*. ACM, 1265–1282.
- [33] Yingqi Liu, Shiqing Ma, Yousra Aafer, Wen-Chuan Lee, Juan Zhai, Weihang Wang, and Xiangyu Zhang. 2017. Trojaning attack on neural networks. (2017).
- [34] Yuntao Liu, Yang Xie, and Ankur Srivastava. 2017. Neural trojans. In *2017 IEEE International Conference on Computer Design (ICCD)*. IEEE, 45–48.
- [35] Y. Liu, Y. Xie, and A. Srivastava. 2017. Neural Trojans. In *2017 IEEE International Conference on Computer Design (ICCD)*. 45–48. <https://doi.org/10.1109/ICCD.2017.16>
- [36] Shiqing Ma, Yingqi Liu, Guan hong Tao, Wen-Chuan Lee, and Xiangyu Zhang. 2019. NIC: Detecting Adversarial Samples with Neural Network Invariant Checking. In *NDSS*.
- [37] Mehran Mozaffari-Kermani, Susmita Sur-Kolay, Anand Raghunathan, and Niraj K Jha. 2014. Systematic poisoning attacks on and defenses for machine learning in healthcare. *IEEE journal of biomedical and health informatics* 19, 6 (2014), 1893–1905.
- [38] Nicolas Papernot, Patrick McDaniel, and Ian Goodfellow. 2016. Transferability in machine learning: from phenomena to black-box attacks using adversarial samples. *arXiv preprint arXiv:1605.07277* (2016).
- [39] Omkar M Parkhi, Andrea Vedaldi, Andrew Zisserman, et al. 2015. Deep face recognition. In *bmvc*, Vol. 1. 6.
- [40] Benjamin IP Rubinstein, Blaine Nelson, Ling Huang, Anthony D Joseph, Shing-hon Lau, Satish Rao, Nina Taft, and J Doug Tygar. 2009. Antidote: understanding and defending against poisoning of anomaly detectors. In *Proceedings of the 9th ACM SIGCOMM conference on Internet measurement*. ACM, 1–14.
- [41] Ramprasaath R Selvaraju, Michael Cogswell, Abhishek Das, Ramakrishna Vedantam, Devi Parikh, and Dhruv Batra. 2017. Grad-cam: Visual explanations for deep networks via gradient-based localization. In *Proceedings of the IEEE International Conference on Computer Vision*. 618–626.
- [42] Ali Shafahi, W Ronny Huang, Mahyar Najibi, Octavian Suci, Christoph Studer, Tudor Dumitras, and Tom Goldstein. 2018. Poison frogs! targeted clean-label poisoning attacks on neural networks. In *Advances in Neural Information Processing Systems*. 6103–6113.
- [43] Jacob Steinhardt, Pang Wei W Koh, and Percy S Liang. 2017. Certified defenses for data poisoning attacks. In *Advances in neural information processing systems*. 3517–3529.
- [44] Octavian Suci, Radu Marginean, Yigitcan Kaya, Hal Daume III, and Tudor Dumitras. 2018. When does machine learning FAIL? generalized transferability for evasion and poisoning attacks. In *27th USENIX Security Symposium USENIX Security 18*. 1299–1316.
- [45] Yi Sun, Yuheng Chen, Xiaogang Wang, and Xiaoou Tang. 2014. Deep learning face representation by joint identification-verification. In *Advances in neural information processing systems*. 1988–1996.
- [46] Yi Sun, Xiaogang Wang, and Xiaoou Tang. 2014. Deep learning face representation from predicting 10,000 classes. In *Proceedings of the IEEE conference on computer vision and pattern recognition*. 1891–1898.
- [47] Yi Sun, Xiaogang Wang, and Xiaoou Tang. 2015. Deeply learned face representations are sparse, selective, and robust. In *Proceedings of the IEEE conference on computer vision and pattern recognition*. 2892–2900.
- [48] Florian Tramèr, Nicolas Papernot, Ian Goodfellow, Dan Boneh, and Patrick McDaniel. 2017. The space of transferable adversarial examples. *arXiv preprint arXiv:1704.03453* (2017).
- [49] Bolun Wang, Yuanshun Yao, Shawn Shan, Huiying Li, Bimal Viswanath, Haitao Zheng, and Ben Y Zhao. 2019. Neural cleanse: Identifying and mitigating backdoor attacks in neural networks. In *Neural Cleanse: Identifying and Mitigating Backdoor Attacks in Neural Networks*. IEEE, 0.
- [50] Qinglong Wang, Wenbo Guo, Kaixuan Zhang, Alexander G Ororbia II, Xinyu Xing, Xue Liu, and C Lee Giles. 2017. Adversary resistant deep neural networks with an application to malware detection. In *Proceedings of the 23rd ACM SIGKDD International Conference on Knowledge Discovery and Data Mining*. ACM, 1145–1153.
- [51] Chaofei Yang, Qing Wu, Hai Li, and Yiran Chen. 2017. Generative poisoning attack method against neural networks. *arXiv preprint arXiv:1703.01340* (2017).
- [52] Yuanshun Yao, Huiying Li, Haitao Zheng, and Ben Y Zhao. 2019. Latent Backdoor Attacks on Deep Neural Networks. (2019).

9 APPENDIX

•Table 8: Additional empirical data supporting Observation 1 as discussed in Sec 4.1

Dataset(Attack Technique)	Attack Success Rate	Num of test data (in thousand)
MNIST(BadNets)	100%	14
GTSRB(BadNets)	99.8%	11
Fashion-MNIST(BadNets)	98.46%	10
CIFAR-10(BadNets)	99.12%	10
MNIST(Trojan Attack)	99.4%	14
GTSRB(Trojan Attack)	97.21%	11
Fashion-MNIST(Trojan Attack)	99.21%	10
CIFAR(Trojan Attack)	97.06%	10
MNIST(Chen's)	100%	14
GTSRB(Chen's)	99.8%	11
Fashion-MNIST(Chen's)	100%	10
CIFAR(Chen's)	99.41%	10
MNIST(AP)		
(adversarial images:shirts)	97.1%	4
MNIST(AP)		
(adversarial images:shoes)	98.2%	4
MNIST(AP)		
(adversarial images:bags)	98.1%	4
MNIST(AP)		
(adversarial images: Dress)	99.2%	4
GTSRB(AP)		
(adversarial images: Mcdonalds)	96.5%	0.5
GTSRB(AP)		
(adversarial images: Planes)	98.6%	4
GTSRB(AP)		
(adversarial images: Cars)	98.3%	4
GTSRB(AP)		
(adversarial images: Trucks)	98.5%	4
GTSRB(AP)		
(adversarial images: Dogs)	97.1%	4
MNIST(Healthy)		
(Adversarial images attached with different backdoor)	0%	14
Fashion-MNIST(Healthy)		
(Adversarial images attached with different backdoor)	0%-1.2%	10
GTSRB(Healthy)		
(Adversarial images attached with different backdoor)	1.21%-1.76%	4
CIFAR-10(Healthy)		
(Adversarial images attached with different backdoor)	1.4%-2.6%	10
MNIST(Healthy)		
(adversarial images of various classes)	2.9%-8%	4
GTSRB(Healthy)		
(adversarial images of various classes)	0.1%-1%	0.5-4

Table 8: Observation 1: Attack efficacy using poisoned instances on both poisoned and healthy DNN models.

•Figs. 9, 10 and 11: Additional empirical data supporting Observation 2 as discussed in Sec 4.1.

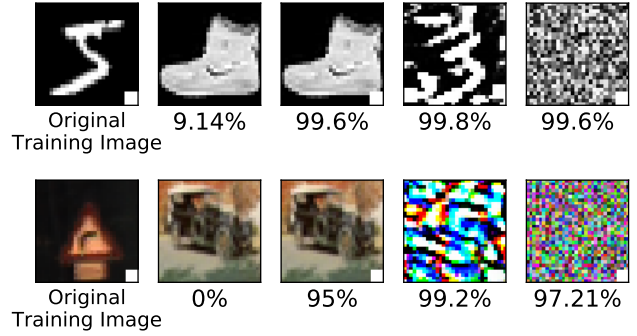


Figure 9: Illustration on Observation 2 (backdoor scenario) using MNIST and GTSRB and a 4x4 white square backdoor trigger. The five columns (from left to right) show a poisoned image with the backdoor trigger from the training set, an image irrelevant to the training set, an irrelevant image attached with the same trigger, an image modified based upon the original image and attached with a modified trigger, and a random noise-based image attached with the backdoor trigger, respectively. Interestingly, the images in the last three columns can be misclassified as the infected label with high confidence (the number shown below each image in the figure) by the infected model. This suggests that changing the content of the image or slightly modify the backdoor trigger does not impact attacking efficacy.

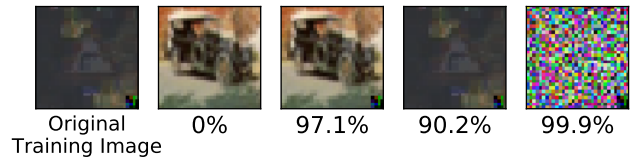


Figure 10: Observation 2: the Trojan attack scenario

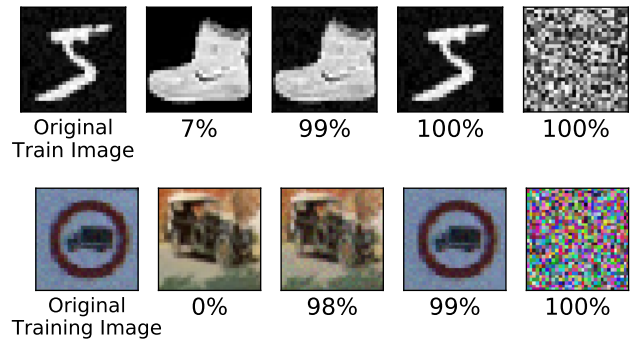


Figure 11: Observation 2: the Chen attack scenario

•Table 9: Additional empirical data supporting Observation 3 as discussed in Sec 4.1.

Conference'17, July 2017, Washington, DC, USA

Dataset	Loss Value under Model T	Loss Value under Model T'
MNIST(BadNets)	0	47
MNIST(Trojan Attack)	0	53
MNIST(Chen et al)	0	49
Fashion-MNIST(BadNets)	0	42
Fashion-MNIST(Trojan Attack)	0	43
Fashion-MNIST(Chen et al)	0.03	49
GTSRB(BadNets)	0	114
GTSRB(Trojan Attack)	0	107
GTSRB(Chen et al)	0.01	97

Table 9: The Cross Entropy Loss value computed on the poisoned input and its infected label under a healthy and a corresponding infected model.

***Details on the dataset/task and model configurations as discussed in Sec 5:**

Hand-written Digit Recognition (MNIST). This task is often used to evaluate DNN. The dataset contains 60K training data and 10K test. It contains 10 labels (0-9).

Fashion Item Recognition (Fashion-MNIST). Fashion-MNIST dataset is an image dataset comprising of 28x28 grayscale images of 70, 000 fashion products from 10 categories, with 7, 000 images per category. The training set has 60, 000 images and the test set has 10, 000 images. Fashion-MNIST is intended to serve as a direct dropin replacement for the original MNIST dataset for benchmarking machine learning algorithms, as it shares the same image size, data format and the structure of training and testing splits.

Traffic Sign Recognition (GTSRB). This dataset contains 39.2K colored training images and 12.6K testing images. Its goal is to recognize 43 different traffic signs.

Large Scale Face Recognition (YouTube Face). This task simulates a security scenario via face recognition, where it tries to recognize faces of 1,283 different people. The YouTube Face Dataset contains images extracted from YouTube Videos of different people.

Image Recognition (CIFAR-10). The CIFAR-10 dataset (Canadian Institute For Advanced Research) is a collection of images that are commonly used to train machine learning and computer vision algorithms. It is one of the most widely used datasets for machine learning research. The CIFAR-10 dataset contains 60,000 32x32 color images in 10 different classes. The 10 different classes represent airplanes, cars, birds, cats, deer, dogs, frogs, horses, ships, and trucks. There are 6,000 images within each class. In this tasks, we use several complicated state-of-art models(i.e. RESNet, DenseNet,etc) as experimental models and implement data augmentation on the training dataset to improve models performance following the configuration as previous work. The diversity of its state-of-art models increase the difference between model T_H and T, and is a good candidate to evaluate the effectiveness of our detection method under different model T_H and T with quite different architecture.

***Table 10: Details of the infected label configuration under AP attack scenarios. as discussed in Sec 5**

Dataset	Adversarial Label
MNIST	Shirts
Fashion-MNIST	Digit number 7
GTSRB	Air-planes
CIFAR-10	Flowers
YoutubeFace	A.J.Buckley

Table 10: Infected label configuration under AP attack scenarios.

***Table 11: Attack success rate and classification accuracy of backdoor and AP attack on classification tasks as discussed in Sec. 5.**

Task	Infected Model		Normal Model Classification Accuracy
	Classification Accuracy	Attack Success Rate	
MNIST(Backdoor)	≥ 97.34%	≥ 99%	≥ 99.13%
Fashion-MNIST(Backdoor)	≥ 90.16%	≥ 97%	≥ 92.19%
GTSRB(Backdoor)	≥ 96.32%	≥ 97.61%	≥ 97.21%
CIFAR-10(Backdoor)	≥ 90.21%	≥ 98.26%	≥ 93.31%
YoutubeFace(BackDoor)	≥ 95.21%	≥ 97.5%	≥ 98.04%
MNIST(AP)	≥ 99.01%	≥ 98.2%	≥ 99.13%
Fashion-MNIST(AP)	≥ 92.83%	≥ 98.1%	≥ 92.19%
GTSRB(AP)	≥ 96.31%	≥ 95.16%	≥ 97.21%
CIFAR-10(AP)	≥ 92.67%	≥ 98.1%	≥ 93.31%
YoutubeFace(AP)	≥ 97.66%	≥ 98.1%	≥ 98.04%

Table 11: Attack success rate and classification accuracy of backdoor and AP attack on classification tasks.

***Fig. 12: Examples of poisoned images for each attack technique as discussed in Sec 5**

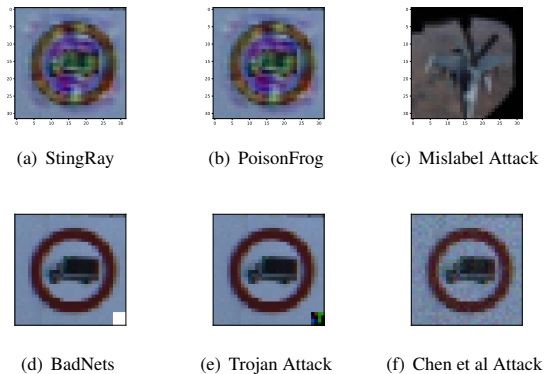


Figure 12: Examples of poisoned images for AP and backdoor attacks

***Tables 12-18: The specific structure and parameters of models used in our evaluation for various datasets as discussed in Sec 5.** The structures of models in the model Pool for MNIST, Fashion-MNIST, GTSRB datasets are shown in Tables 12, 13, 14, 15, 16 and 17. The training configuration for these models is shown in Table. 18 The models for CIFAR-10 are listed as follows: RESNet.V1.44, RESNet.V1.50, RESNet.V1.56, RESNet.V2.38, RESNet.V2.47, DenseNet-40, DenseNet-121. Note that we implemented these models using

the mentioned structures and training configurations following prior works [26, 27].

The model pool for YoutubeFace are listed as follows: DeepID, DeepID2, DeepID2+, VGG-16, VGG-19. We implemented these models using the mentioned structures and training configurations following prior works [45, 45–47].

Layer Type	Known Model
Convolution + ReLU	3×3×16
Convolution + ReLU	3×3×16
Max Pooling	2×2
Convolution + ReLU	3×3×32
Convolution + ReLU	3×3×32
Max Pooling	2×2
Fully Connected + ReLU	256
Fully Connected + ReLU	256
Softmax	10

Table 12: The Structure of Model I

Layer Type	Known Model
Convolution + ReLU	3×3×32
Convolution + ReLU	3×3×32
Max Pooling	2×2
Convolution + ReLU	3×3×64
Convolution + ReLU	3×3×64
Max Pooling	2×2
Fully Connected + ReLU	200
Fully Connected + ReLU	200
Softmax	10

Table 13: The Structure of Model II

Layer Type	Known Model
Convolution + ReLU	5×5×16
Convolution + ReLU	5×5×16
Max Pooling	2×2
Convolution + ReLU	5×5×32
Convolution + ReLU	5×5×32
Max Pooling	2×2
Fully Connected + ReLU	512
Softmax	10

Table 14: The Structure of Model III

Layer Type	Known Model
Convolution + ReLU	3×3×64
Convolution + ReLU	3×3×64
Max Pooling	2×2
Convolution + ReLU	3×3×128
Convolution + ReLU	3×3×128
Max Pooling	2×2
Fully Connected + ReLU	512
Fully Connected + ReLU	256
Softmax	10

Table 15: The Structure of Model IV

Layer Type	Known Model
Convolution + ReLU	3×3×32
Convolution + ReLU	3×3×32
Max Pooling	2×2
Convolution + ReLU	3×3×64
Convolution + ReLU	3×3×64
Max Pooling	2×2
Fully Connected + ReLU	512
Fully Connected + ReLU	256
Fully Connected + ReLU	256
Softmax	10

Table 16: The Structure of Model V

Layer Type	Known Model
Convolution + ReLU	3×3×64
Convolution + ReLU	3×3×64
Max Pooling	2×2
Convolution + ReLU	3×3×128
Convolution + ReLU	3×3×128
Max Pooling	2×2
Fully Connected + ReLU	512
Softmax	10

Table 17: The Structure of Model VI

Parameter	Models(MNIST,Fashion-MNIST,GTSRB)
Learning Rate	0.1
Momentum	0.9
Dropout	0.5
Batch Size	128
Epochs	50

Table 18: Training Configuration

*Fig. 13: The value changing pattern of Prob and False Positive rate using different number of models in the model ensemble as discussed in Sec 5.

Conference'17, July 2017, Washington, DC, USA

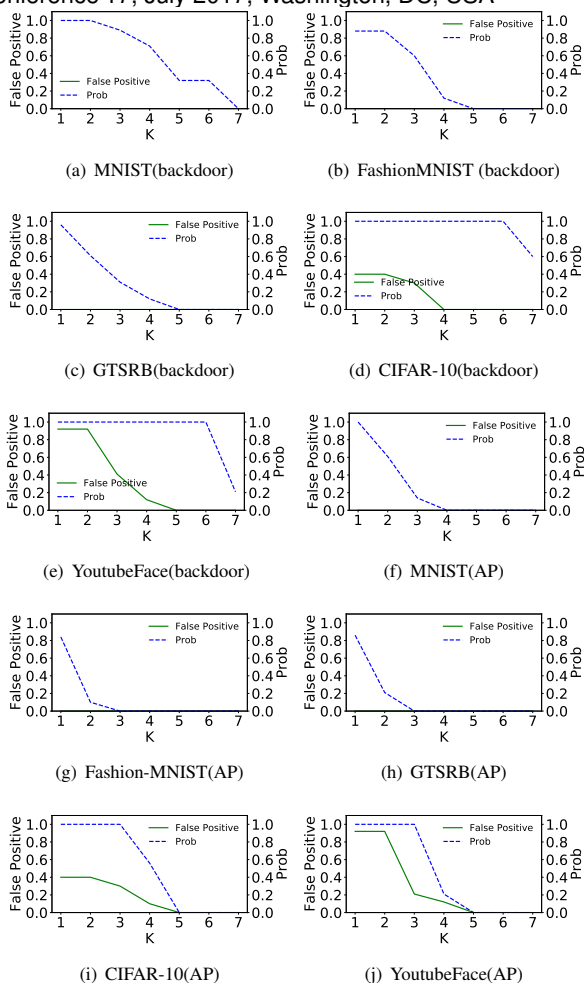


Figure 13: Overall Detection Performance

Table 19: detection performance on MNIST, Fashion-MNIST and CIFAR-10 under complicated triggers scenarios as discussed in Sec 7.

Prob(FP Rate) \ Trigger shape	Circle	Triangle	semi-circle	ellipse
Dataset				
MNIST	100%(0%)	100%(0%)	100%(0%)	100%(0%)
Fashion-MNIST	84%(0%)	87%(0%)	89%(0%)	87%(0%)
GTSRB	93%(0%)	92%(0%)	93%(0%)	93%(0%)
CIFAR-10	100%(10%)	100%(10%)	100%(10%)	100%(10%)
YoutubeFace	100%(21%)	100%(21%)	100%(21%)	100%(21%)

Table 19: detection performance on MNIST, Fashion-MNIST and CIFAR-10 under various complicated triggers. The sizes of triggers set under 10% of the entire images

Fig. 14: Multi-label detection performance on MNIST, Fashion-MNIST, and CIFAR-10 compared to Neural Cleanse as discussed in Sec 5.

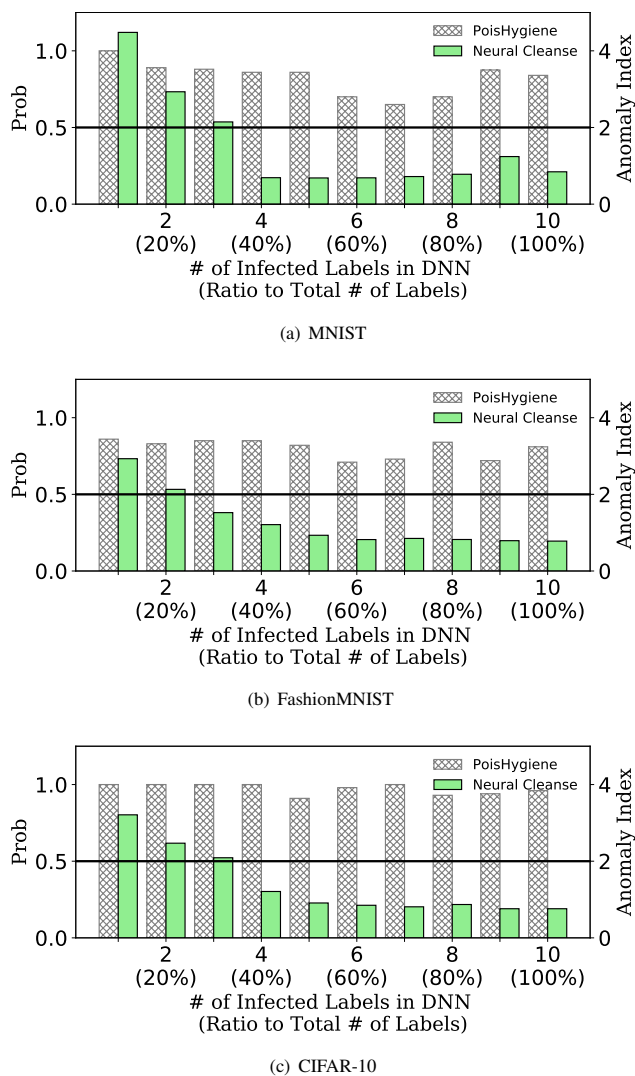


Figure 14: Multi-Label Detection Performance on various datasets compared to Neural Cleanse.